

PROCEEDINGS OF SPIE

SPIDigitalLibrary.org/conference-proceedings-of-spie

Spatial resolution in three-dimensional photo-acoustic reconstruction

Minghua Xu, Lihong V. Wang

Minghua Xu, Lihong V. Wang, "Spatial resolution in three-dimensional photo-acoustic reconstruction," Proc. SPIE 5320, Photons Plus Ultrasound: Imaging and Sensing, (12 July 2004); doi: 10.1117/12.530475

SPIE.

Event: Biomedical Optics 2004, 2004, San Jose, CA, United States

Spatial resolution in three-dimensional photo-acoustic reconstruction

Minghua Xu and Lihong V. Wang*

Optical Imaging Laboratory, Department of Biomedical Engineering,
Texas A&M University, 3120 TAMU, College Station, Texas 77843-3120

ABSTRACT

We present an analytic explanation of the spatial resolution in three-dimensional photo-acoustic (also called opto-acoustic or thermo-acoustic) reconstruction. Based on rigorous reconstruction formulas, we analytically derive the point-spread functions (PSFs) for three types of specific recording geometries, including spherical, planar, and cylindrical surfaces. The PSFs as a function of the bandwidth of the measurement system and the finite size of the detector aperture, as well as the discrete sampling effect on the reconstruction, are investigated. The analyses clearly reveal that the dependence of the PSFs on the bandwidth of all of the recording geometries shares the same space-invariant expression while the dependence on the aperture size of the detector differs. The bandwidth affects both axial and lateral resolution; in contrast, the detector aperture blurs the lateral resolution greatly but the axial resolution only slightly. Under-sampling in the measurement causes significant aliasing artifacts in the reconstruction. A general sampling strategy to avoid aliasing is proposed.

Keywords: Spatial resolution, Photoacoustic tomography, Reconstruction, Imaging

1. INTRODUCTION

Photo-acoustic (PA) reconstruction, or tomography, has great potential for applications in the biomedical field.^{1,2} With this technique, an electromagnetic (EM) pulse, such as an optical-wave or microwave pulse, illuminates a sample. The energy absorbed by the sample produces a small temperature rise and then induces a pressure inside the sample through thermal expansion. This initial pressure acts as an acoustic source and generates further acoustic wave propagation. The outgoing acoustic waves can be detected by ultrasound transducers positioned outside the sample. All of the measured data are used to reconstruct the initial pressure, and finally, a photoacoustic image is obtained. This technique combines the spatial resolution of ultrasonic waves and the contrast of EM absorption.

In practice, many factors can affect the spatial resolution of PA imaging. Acoustic heterogeneity can blur the reconstructed image. Acoustic attenuation limits the achievable high-frequency signal since the attenuation increases tremendously in high MHz ultrasound. A limited-angle view also affects spatial resolution due to the lesser amount of raw data. Both the excitation pulse of an EM wave and the bandwidth of the detection system determine the temporal-frequency bandwidth of the detected PA signal. The sensing aperture of the detector can blur the spatial resolution. Aliasing due to under-sampling can cause confusion and serious measurement errors.

In this paper, we present an analytic explanation of the spatial resolution in three-dimensional photo-acoustic reconstruction. We will discuss the bandwidth-related point-spread function (PSF), the effect of the detector aperture on the spatial resolution, and the discrete sampling effect on the PA reconstruction in Secs. 2, 3, and 4, respectively. Finally, we will present a summary in Sec. 5.

* To whom all correspondence should be addressed. Telephone: 979-847-9040; fax: 979-845-4450; electronic mail: LWang@tamu.edu; URL: <http://oilab.tamu.edu>.

2. BANDWIDTH-RELATED PSF

To investigate the spatial resolution, we use exact reconstruction formulas to derive PSFs related to the temporal-frequency bandwidth. We have studied three recording geometries, including spherical, planar, and cylindrical surfaces.³

Theoretically, with a $\delta(t)$ excitation, the initial pressure $p_0(\mathbf{r}) = A(\mathbf{r})\Gamma(\mathbf{r})$, where $A(\mathbf{r})$ is the EM absorption function and the Gruneisen coefficient $\Gamma(\mathbf{r}) = \beta c^2/C_p$ (C_p —the specific heat, β —the isobaric volume expansion coefficient, and c —sound speed). For convenience, we define the Fourier transform over variable $\bar{t} = ct$ as

$$\bullet(k) = \int \bullet(\bar{t}) \exp(ik\bar{t}) d\bar{t}. \quad (1)$$

We consider a point-detector measurement at position \mathbf{r}_0 :

$$\tilde{p}_d(\mathbf{r}_0, k) = -ik\tilde{H}(k) \iiint d^3r p_0(\mathbf{r}) \tilde{G}_k(\mathbf{r}, \mathbf{r}_0), \quad (2)$$

where $k = 2\pi f/c$ (f —frequency); $\tilde{H}(k)$ denotes the bandwidth of the measured PA signal; and the Green's function $\tilde{G}_k(\mathbf{r}, \mathbf{r}_0) = \exp(ik|\mathbf{r} - \mathbf{r}_0|)/(4\pi|\mathbf{r} - \mathbf{r}_0|)$.

The bandwidth $\tilde{H}(k)$ has two contributors: $\tilde{H}(k) = \tilde{I}_e(k)\tilde{I}_d(k)$, where $\tilde{I}_e(k)$ is the Fourier transform of the temporal-profile of the excitation pulse, and $\tilde{I}_d(k)$ is the bandwidth of the detection system. We can denote $H(t)$ as the temporal profile of $\tilde{H}(k)$. In general, $H(t)$ can be split into even and odd portions as $E(t)$ and $O(t)$, respectively, and, then, the corresponding PSF is found to be

$$\text{PSF}(R) = -\frac{1}{2\pi R} \cdot \frac{dE(R)}{dR}, \quad (3)$$

where R is the distance between the point of observation and the acoustic source. The odd part is cancelled out in the reconstruction.

We take the rectangle-shaped bandwidth as an example, which is cut off at the frequency of f_c . In this case, $H(t)$ is a sinc function as $\text{sinc}(Kt)K/\pi$, where $\text{sinc}(x) = \sin(x)/x$ and $K = 2\pi/\lambda_c$ (λ_c : the cutoff wavelength = $2\pi c/f_c$). We find that the dependence of the PSFs on the bandwidth of all of the recording geometries shares the same space-invariant expression as³

$$\text{PSF}(R) = \frac{K^3}{2\pi^2} \cdot \frac{j_1(KR)}{KR}, \quad (4)$$

where $j_1(\cdot)$ is the first-order spherical Bessel function of the first kind. If the full-width half-maximum (FWHM) of the PSF is used to represent the spatial resolution, in this case, $R_w \approx 0.80\lambda_c$. In an analogy to the Rayleigh criterion, an alternative definition of spatial resolution is the distance between two PSFs when the maximum (positive) of one PSF is at the first minimum (negative) of the second. By this definition, the spatial resolution becomes $R_R \approx 0.92\lambda_c$, which is slightly wider than the FWHM definition. The Rayleigh criterion is more appropriate, however, because negative-valued artifacts are introduced into the reconstruction due to the limited bandwidth.

3. EFFECT OF DETECTOR APERTURE

For simplicity, the measurement with a finite sensing aperture can be written as an integral over the sensing aperture:

$$\tilde{p}'_d(\mathbf{r}_0, k) = \int \int_{\mathbf{r}'} d^2\mathbf{r}' W(\mathbf{r}') \tilde{p}_d(\mathbf{r}_0 + \mathbf{r}', k), \quad (5)$$

where $W(\mathbf{r}')$ is a weighting factor, which represents the contribution from the various surface elements of the detector to the total signal received by the detector.



Figure 1 Schematic of the extension of PSF in (a) a circular scan and (b) a straight-line scan.

The theoretical analyses indicate that the detector aperture only slightly changes the axial resolution but greatly affects the lateral resolution.³ As shown in Fig. 1(a), if the detection scan is along a circle, such as a spherical or cylindrical scan, the lateral extension of the PSF can be estimated by $(r/r_0)\delta$, where r is the distance between the point source and the center of the scan circle, r_0 is the radius of the scan circle, and δ is the diameter of the detector. The closer the point source is to the center, the smaller extension the PSF has. Therefore, the lateral resolution improves when the point source approaches the scan center. As shown in Fig. 1(b), if the detection scan is along a straight line, such as a planar scan or a z -scan in the cylindrical scan, the lateral extension of the PSF approximately equals the diameter of the detector aperture. Therefore, the lateral resolution is blurred by the detector aperture no matter where the point source is.

The combined effects of the temporal-frequency bandwidth and the aperture of the detector on the PSF can be regarded as a complicated convolution of the aperture with the PSF related to the temporal-frequency bandwidth.³

4. DISCRETE SAMPLING EFFECT

In the measurement, the PA waves are acquired at a series of discrete spatial detection positions with a spatial sampling frequency (the inverse of the sampling period), and at each detection position a series of discrete temporal points are sampled with a temporal sampling frequency. According to the sampling theorem, to accurately reconstruct a signal, the sampling frequency must be at least twice the maximum frequency of the signal. Otherwise, aliasing artifacts occur in which the high-frequency components above half the sampling frequency will disguise as low-frequency components.

The recorded PA signal is actually band-limited either in the temporal spectrum or in the spatial spectrum, because of the finite duration of the EM excitation pulse and the finite bandwidth of the detection system as well as the finite sensing aperture of the detector. Therefore, if the PA signal is sampled at the Nyquist frequency (twice the highest frequency of the bandwidth), no frequency information is lost.

In the sampling of temporal signals, an analog anti-aliasing filter is often applied prior to the analog-to-digital (A/D) converter, which filters out frequency information that is higher than half the temporal sampling frequency. In the surface scan, the spatial sampling is dependent on the recording geometries. In general, the main-lobe of the spatial-frequency bandwidth of the detector aperture is cut off at about one over the diameter of the detector aperture. Therefore, if the spatial sampling period is less than half the diameter of the detector, the aliasing related to spatially discrete sampling can be significantly reduced.

Without loss of generality, we can take the planar recording geometry as an example. Assume the recording area is 40 mm \times 40 mm. Consider two spherical absorbers located 10 mm away from the scan plane. As shown in Fig. 2, the solid line is the initial pressure profile through the centers of these two absorbers. Assume that the cutoff frequency of the temporal frequency is 4 MHz and the diameter of the detector is 2 mm. We use the back-projection algorithm⁴ to compute the reconstructions from the measurements with various spatial sampling periods including 4 mm and 1 mm. The profiles of these reconstructions along the line through the centers of the absorbers are plotted as dash lines in Figs. 2(a) and (b), respectively. When the sampling period is much greater than 1 mm, such as the dash line in Fig. 2(a), the reconstruction contains significant aliasing artifacts, in which the object with low amplitude is buried in the aliasing noise. While the reconstruction in Fig. 2(b) is in good agreement with the original profile since the sampling period is sufficient.

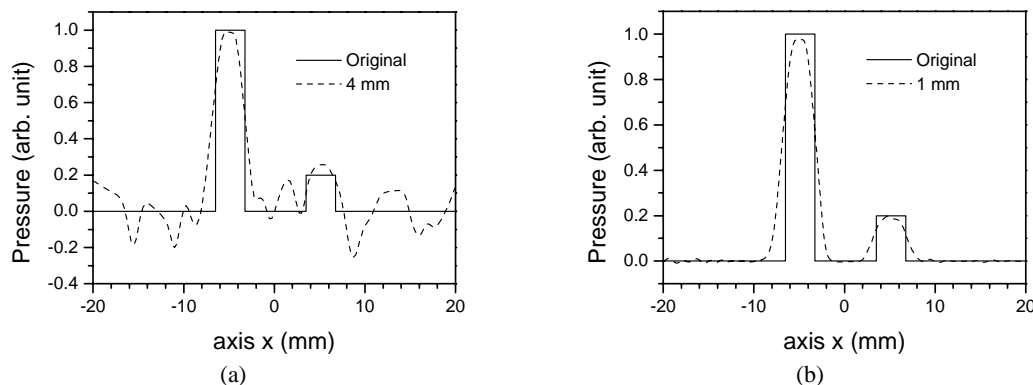


Figure 2 Comparison of the original pressure profiles (solid lines) with the reconstructions (dash lines) from the measurements with spatial sampling periods: (a) 4 mm and (b) 1 mm, respectively.

5. SUMMARY

Spatial resolution is physically limited by the sensing aperture size of the detector and the temporal-frequency bandwidth of the detection system as well as the excitation pulse duration. To avoid aliasing, it is reasonable to let the spatial-sampling period be slightly smaller than half the diameter of the sensing aperture of the detector. However, it is not necessary to let the spatial sampling period be far smaller than one quarter of the diameter of the sensing aperture, because a smaller sampling period increases tremendously the number of the detection positions but does not provide significant improvement in image quality.

ACKNOWLEDGMENTS

This project was sponsored in part by the U.S. Army Medical Research and Materiel Command Grant No. DAMD17-00-1-0455, the National Institutes of Health Grants No. R01 EB000712 and No. R01 NS46214, the National Science Foundation Grant No. BES-9734491, and Texas Higher Education Coordinating Board Grant No. ARP 000512-0063-2001.

REFERENCES

1. M. Xu and L.-H. Wang, "Time-domain reconstruction for thermoacoustic tomography in a spherical geometry," *IEEE Transactions on Medical Imaging* 21 (7), 814–822 (July 2002).
2. X. Wang, Y. Pang, G. Ku, X. Xie, G. Stoica, and L.-H. Wang, "Non-invasive laser-induced photoacoustic tomography for structural and functional imaging of the brain in vivo," *Nature Biotechnology* 21 (7), 803-806 (July 2003).
3. M. Xu and L.-H. Wang, "Analytic explanation of spatial resolution related to bandwidth and detector aperture size in thermoacoustic or photoacoustic reconstruction," *Physical Review E* 67 (5), 056605, 1-15 (May 2003).
4. M. Xu, Y. Xu, and L.-H. Wang, "Time-domain reconstruction algorithms and numerical simulations for thermoacoustic tomography in various geometries," *IEEE Transactions on Biomedical Engineering*, 50 (9), 1086-1099 (September 2003)